

Theoretical Investigation of Buoyancy-driven Cavity Flow by Using Finite Element

Abbas Z. Salman¹, Mohammed A. Fayad², Ahmed Q. Salam³

^{1,2,3}Energy and Renewable Energies Technology Center, University of Technology-Iraq, Baghdad
Email address: 11016@uotechnology.edu.iq¹, 11013@uotechnology.edu.iq², 20307@uotechnology.edu.iq³

Abstract—This research presents a mathematical model (finite element) to calculate the flow due to natural convection and heat transfer in enclosures. In this study, the equations were built according to suppose the flow two-dimensional and steady. Moreover, the equations are adopted from the finite element method and used in the stream function-vorticity form to allow for complex geometries and irregular boundaries.

The two sides of walls (top and bottom) are perfectly insulated and completely conducting. The results from the current model are in agreement with previous published results. The both temperature and flow fields in solid walls at theoretical results of isothermal contour lines were verified by comparing with the useful experimental results. The results of heat transfer are calculated through enclosures containing square and circular cavities. It was found that a large reduction up to 38% can be achieved in the heat transfer rates over walls by using walls including cavities, for the cases studied. For the same area ratio, the results indicated that the enclosures containing square were supplied better insulation when compared to the circular ones. Also, increase the dependence of heat transfer on geometry with increase of Rayleigh number.

Keywords— Finite element, heat transfer, natural convection, enclosures, Rayleigh number.

I. INTRODUCTION

A large size of research efforts has been dedicated to the problem of natural convection heat transfer and buoyancy-driven flows in enclosures, especially during the last two decades. However, the phenomenon occurs in many engineering systems. For example, convective processes in lakes, thermal insulation in buildings, solar collectors, convection in melting chambers, fire and smoke spread in rooms, porous materials and cellular structures. Furthermore, the enclosures problem increases when a solid completely envelops a cavity containing a fluid and possibly interior solids. Problems without interior solids include the heat transfer between the various surfaces of the enclosures. Figure 1 shows the most famous enclosures of this type which are rectangular, parallelepiped cavities, while figure 2 illustrates truncated circular cylinder cavities (walls, cement blocks, cellular cavities).

Buoyancy-driven flow and natural convection heat transfer in enclosures can occur because of complex interaction between finite-size fluid in thermal contact with all walls that confine it, i.e., there is an interaction between the convection in the fluid-filled-cavity and conduction in the walls surrounding it. Previous studies were concerned just with two types of idealized boundary conditions, namely, enclosures with perfectly insulated connecting walls and those with perfectly conducting connecting walls.

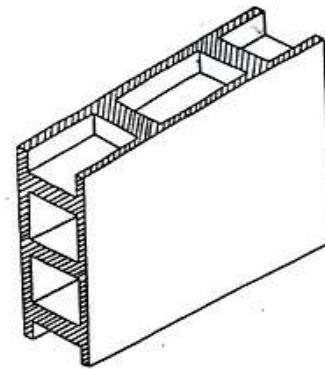


Fig. 1. Rectangular parallelepiped cavities.

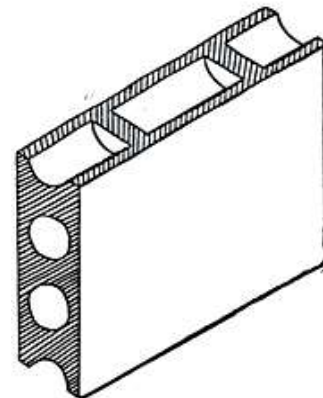


Fig. 2. Truncated circular cylinder cavities.

The work by Chan and Banerjee [1] measured natural convection in rectangular enclosures with perfectly insulated connecting walls. The marker and cell finite difference method (MAC) was used. A close match to the perfectly insulated connecting walls requires that the thermal conductivity of the wall material be at least an order of magnitude smaller than the thermal conductivity of the fluid. Subsequently, most of the engineering applications are concerned with air as a working fluid, such wall materials do not exist ($k^* < 1$), and hence the perfectly insulated connecting walls are not attainable for air. In contrast, a close match to the perfectly conducting connecting walls can be realized by using a relatively thin flat sheet of metal [1], but not all engineering problems can be modeled as enclosures having perfectly walls. Therefore, it becomes necessary to look for another more realistic class of wall boundary conditions.

Three recent, remotely related studies, El-Sherbiny, et al. [2], Meyer et al. [3] and Mallinson [4], considered the effect of conduction in connecting walls only, Fig. (3). Kim and

Viskanta [5], reported a numerical and experimental study of natural convection in a two-dimensional rectangular enclosures with all walls having finite conductance containing rectangular cavity. They used simplified boundary conditions on the solid-fluid interface together with a finite difference numerical model, to simplify the calculations. There are some physical situations where heat conduction in the enclosure walls material must be considered. It has been recognized that the wall conductance has an important effect on convection heat transfer in the cavity, El-Sherbiny et al. [2]. Wall conduction effect is also obvious in cellular and porous materials as well as cellular structures applications, Kim and Viskanta [5].

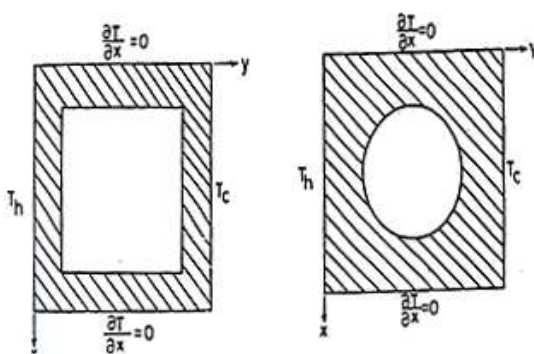
To the authors knowledge the heat and fluid flow in non-rectangular cavities with walls having finite conductance were not studied. The main objectives of the present work are:

1. The use of finite element method which allows irregular mesh over non-rectangular cavities to be implementing.
2. Examination of the natural convection heat transfer and buoyancy-driven flow in enclosures heated from a side with all walls having finite conductance.
3. Investigation of the effect of cavity geometries on the thermal insulation of enclosures having the same area ratio (cavity to block area). The heat transfer rates through enclosures containing square cavities are compared with those containing circular ones having the same cavity-to-block area ratio.

II. PROBLEM FORMULATION

The basic assumptions made in the present analysis are:

- The heat transfer processes and fluid flow are steady, two-dimensional and laminar.
- All physical properties are constant except density, whose variation with temperature is accounted only in the buoyancy term, using the Boussinesq approximation. It states that, for buoyancy-driven flow, when $(T-T_0) \ll T_0$, the density can be approximated as $\rho = \rho_0[1-(T-T_0) / T_0]$. This approximation is used to relate the energy and momentum equations through the buoyancy term.
- Viscous heat dissipation is negligible in comparison with conduction and convection.
- Vertical enclosure is considered, figures 3-a and 3-b



(a) Containing square cavity. (b) Containing circular cavity.
Fig. 3. Enclosure with all walls having finite conductance.

III. BASIC EQUATIONS

The basic equations are used in the stream function vorticity form in order to avoid the need for solving the Poisson equation for the pressure. Variables are normalized using L for length, (T_h-T_c) for temperature and thermal diffusivity α for stream function. The following dimensionless variables are defined:

$$X = \frac{x}{L}, Y = \frac{y}{L}, N = \frac{n}{L}, \theta = (T-T_c) / (T_h-T_c)$$

$$\Psi = \frac{\psi}{\alpha}, U = \frac{u}{\alpha}, V = \frac{v}{\alpha}, \omega = \frac{\omega}{L^2}, Ra^* = \frac{g\beta(T_h-T_c)L^3}{\alpha}, Pr = \nu/\alpha$$

The Jacobian

$$J(A,B) = \left(\frac{\partial A}{\partial X} \frac{\partial B}{\partial Y} - \frac{\partial A}{\partial Y} \frac{\partial B}{\partial X} \right)$$

The dimensionless variables can be substituting in the basic equations of vorticity, energy and boundary conditions, the following governing equations are obtained:

a) For the Fluid-Filled Cavity:

$$J(\theta, \Psi) - \nabla^2 \theta = 0 \tag{1}$$

$$J(\Omega, \Psi) - Pr \nabla^2 \Omega = Pr Ra^* \frac{\partial \theta}{\partial Y} \tag{2}$$

$$-\nabla^2 \Psi = \Omega \tag{3}$$

$$U = \frac{\partial \Psi}{\partial Y} \tag{4}$$

$$-V = \frac{\partial \Psi}{\partial X} \tag{5}$$

$$K \nabla^2 \theta = 0 \tag{6}$$

$$\Psi_b = -2\Psi_b / (\Delta N)^2 \tag{7}$$

$$\Psi = 0, U = 0, V = 0 \tag{8}$$

$$\frac{\partial \theta}{\partial X} \Big|_{(0,y)} = 0 \tag{9}$$

$$\frac{\partial \theta}{\partial X} \Big|_{(1,y)} = 0 \tag{10}$$

$$\theta(x,0) = 1 \tag{11}$$

$$\theta(x,1) = 0 \tag{12}$$

The dimensionless heat transfer rate (Q^*), which is defined as the ratio of heat transfer with cavity to heat transfer at zero area ration, ($A^* = 0$) i.e. without cavity is given by:

$$Q^* = \frac{\partial \theta}{\partial Y} \Big|_{Y=0}$$

$$Q^* = \int_0^1 \frac{\partial \theta}{\partial Y} \Big|_{(y=0)} dx \tag{13}$$

$$Nu = -K(dx.1) \frac{\partial \theta}{\partial Y} \Big|_{cavity\ wall} / (-K(dx.1) \left(\frac{T_h - T_c}{L_1} \right)) \tag{14}$$

$$Nu = \frac{L_1}{L} \frac{\partial \theta}{\partial Y} \Big|_{cavity\ wall}$$

The distribution of the local Nusselt number on the hot wall of the cavity is calculated based on the outer temperature difference across the enclosure boundary and the cavity length L_1 , then;

$$Nu = \frac{L_1}{L} \int_a^b \left. \frac{\partial \theta}{\partial Y} \right|_{cavity\ wall} dx \quad (15)$$

$$a = (L - L_1) / 2L \text{ and } b = 1 - a$$

IV. FINITE ELEMENT FORMULATION

The finite element method is used here to accommodate the complex geometries, non-homogeneous material and complicated boundary conditions. Piecewise approximation together with an interpolation function is used to approximate the field variables (stream function, vorticity and temperature) over the element in terms of its nodal values. Here two-dimensional triangular elements are used. For the present investigation, approximately 20 by 20 elements are used. More elements are considered for circular cavity problem. The general field variable r is considered linear in both X and Y in each element;

$$\Gamma(X, Y) = a_1 + a_2X + a_3Y \quad (16)$$

The characteristics matrices are derived using the usual Galerkin's procedure [6]. Element equations are assembled to obtain the overall set of equations for the total domain. Iterative solution is carried out until a relative correction of less 1% is achieved.

V. RESULTS AND DISCUSSION

Computations are carried out one cell only which represents a square enclosure containing a square or circular cavity. Figure (3-a) and (3-b) solutions are obtained for the simplified boundary conditions of insulated connecting walls or perfectly conducting connecting walls as well as for the finite wall conductance conditions. Results include contour lines for stream functions and temperatures in addition to local and average Nusselt numbers at various values of Rayleigh numbers. Two values of the thermal conductivity ratio (k^*) are used namely 10 and 7.4 and an ratio (A^*) of 0.36 values of thermal conductivity ratio correspond to the clay-to-air thermal conductivity ratio.

i) Enclosure with Perfectly Insulated Connecting Walls

Figure (4-a) and (4-b) show the dimensionless isothermal contour lines for different values of Rayleigh numbers namely 10^3 and 10^5 . The dimensionless isothermal is worth to notice that dimensionless isothermal contour line of 0.5 divides the domain to two equal areas. Furthermore, the area above the dimensionless isothermal line 0.5 (upper left area) denotes the hot region and area under the dimensionless isothermal line 0.5 (lower right area) denotes the cold region. In addition, it can be shown that as the value of Rayleigh number increases the cold area moves from the right half of the enclosure towards the bottom. In other words, for this geometry and the given boundary condition the cold area rotates in clockwise direction as the Rayleigh number increases.

Dimensionless stream function contours are shown in figure (5-a) and (5-b). It can be observed that the cell secondary flow appears at the higher value of Rayleigh number.

The mid-plane velocity components at different values of Rayleigh number are shown in figures (6-a) and (6-b).

The distribution of the local Nusselt number at the heated wall is shown in figure 7. It can be noticed that the Nusselt number attains its highest value near the bottom. This is caused by the cold fluid, which moves from cold walls and impinges on the hot wall near the base. Comparison of the average Nusselt number with the published results is given in table I which agrees very well with the published ones.

ii) Enclosure with Finite Wall Conduction:

The dimensionless isothermal contour lines in both walls and fluid with dimensionless temperature difference of 0.1 are shown in figures (8-a) and (8-b). The boundary surfaces of the fluid are indicated by dash lines. The results show the same trend as those given in figures (4-a) and (4-b).

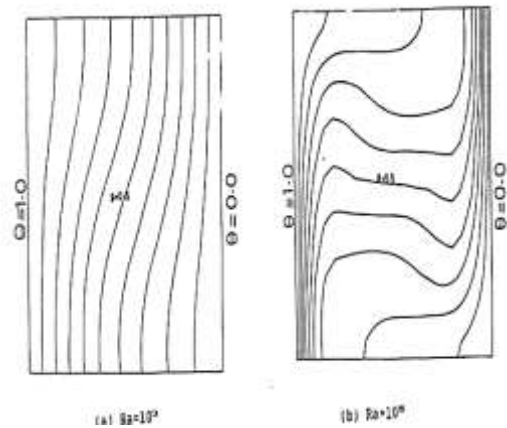


Fig. 4. Dimensionless isothermal contour lines for enclosure with perfectly insulated connecting walls, Pr=0.71, AS1=1.0, $\Delta\theta = 0.1$.

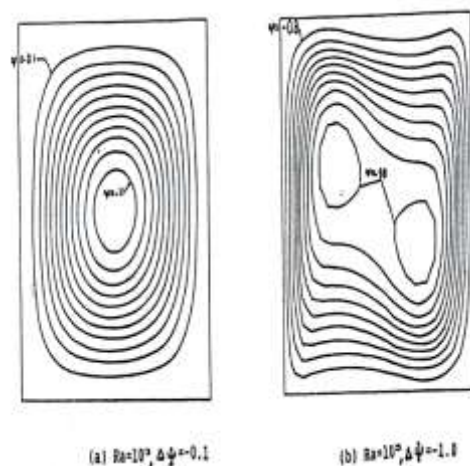


Fig. 5. Dimensionless streamlines for enclosure with perfectly insulated connecting walls, Pr=0.71, AS1=1.0, $\Delta\psi = 1=90^\circ$.

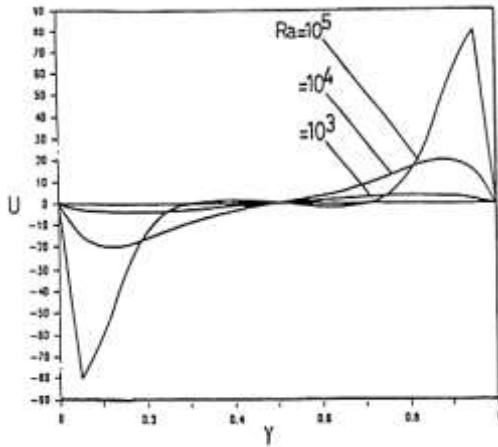


Fig. 6-a. Dimensionless vertical velocity components at horizontal mid-plane, for enclosure with perfectly insulated connecting walls, $Pr=0.71$, $AS1=1.0$, and $\phi=90^\circ$.

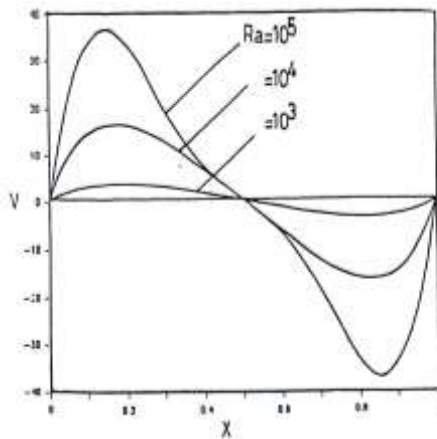


Fig. 6-b. Dimensionless horizontal velocity components at horizontal mid-plane, for enclosure with perfectly insulated connecting walls, $Pr=0.71$, $AS1=1.0$, and $\phi=90^\circ$.

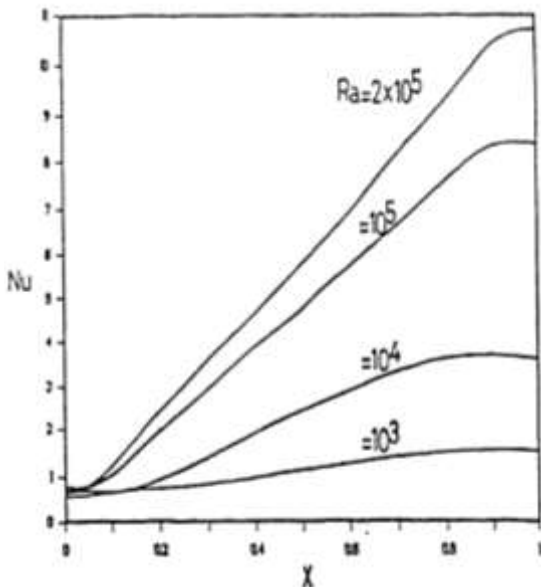


Fig. 7. Distribution of the local Nusselt numbers at the heated wall for enclosure with perfectly insulated connecting walls, $Pr=0.71$, $AS1=1.0$, and $\phi=90^\circ$.

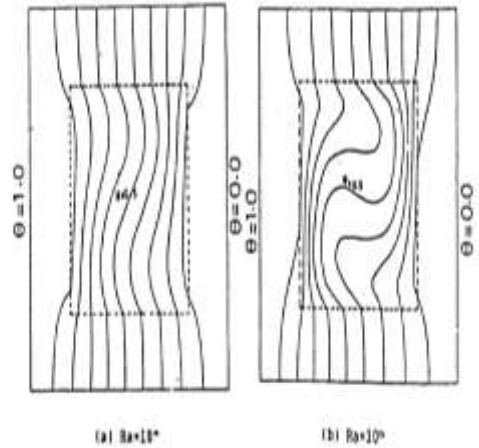


Fig. 8. Dimensionless isothermal contour lines for enclosure containing a square cavity, $Pr=0.71$, $K^*=10.0$, $A^*=0.36$, $AS=1.0$, $AS1=1.0$, $E=0$, $\phi=90^\circ$ and $\Delta\theta=0.1$.

TABLE I. Comparison of the average Nusselt at heated wall with the other published results. For enclosure with perfectly insulated connection walls, $Pr=0.71$, $AS1=1.0$, $\phi=90^\circ$.

Ref.	Ra		
	10^3	10^4	10^5
[7]	1.119	2.520	4.594
[8]	1.117	2.242	4.523
[9]	1.119	2.292	4.638
[10]	1.120	2.268	4.623
[11]	1.120	2.240	4.510
[12]	1.118	2.244	4.525
present	1.122	2.288	4.715

To verify the model, the isothermal contour line of 0.5 at Rayleigh number 0.46×10^6 of the present calculation are compared with the available experimental contour lines [7]. The comparison of figure (9) shows excellent agreement near the middle of the cavity. In addition, near the boundary of the cavity, the slope of the isothermal contour lines of the present work compares well with the experimental ones with some discrepancy in θ magnitudes. The discrepancy could be due to insufficient fine elements near the boundary or the dependence of the thermal fluid properties on temperature. Moreover, similar plots show better agreement at smaller values of Rayleigh number.

iii) Square Enclosure Containing Circular Cavities

Figures (10-a) and (10-b) show dimensionless isothermal lines for Rayleigh numbers 10^4 and 10^5 in both wall and fluid with dimensionless temperature difference of 0.1. The boundary surface of the fluid is indicated by dashed lines. It can be observed that natural convection causes the temperature profile in fluid to deviate from the linear one. As Rayleigh number increases more deviation is noticed.

One of the major concerns of the present work is to compare results obtained for cavities with different geometries [13,14]. Table II shows a comparison of the average dimensionless rate of heat transfer for square and circular

cavities. It shows that the heat transfer through the enclosure containing square cavity is less than through circular one for the same area ration thermal conductivity ratio.

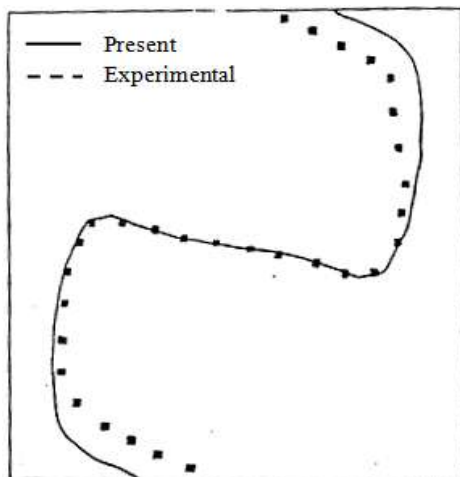


Fig. 9. Dimensionless of the isothermal contour lines of 0.5 with the published results, [5] for the enclosure containing a square cavity, $Ra^* = 0.64 \times 10^6$, $Pr = 0.71$, $K^* = 7.4$, $A^* = 0.36$, $AS = 1.0$, $AS1 = 1.0$, $\theta = 90^\circ$.

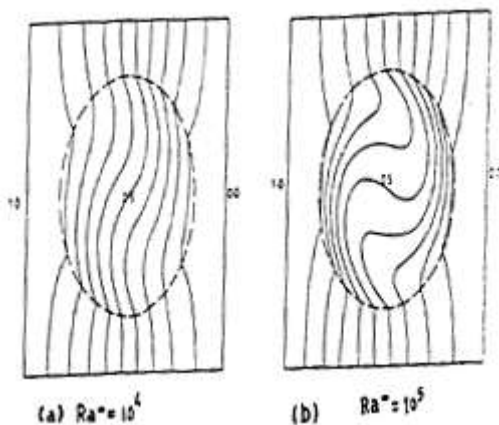


Fig. 10. Dimensionless of the isothermal contour lines enclosure containing a circular cavity, $Pr = 0.71$, $K^* = 7.4$, $A^* = 0.36$, $AS = 1.0$, $AS1 = 1.0$, $\theta = 90^\circ$, $\theta1 = 90^\circ$ and $E = 0$.

TABLE II. Comparison of total dimensionless heat transfer rate at the heated wall for the enclosure containing square cavity to that of the enclosure containing circular cavity, $pr = 0.71$, $A^* = 0.36$, $k^* = 10$, $AS = 1.0$, $AS1 = 1.0$, $\theta = 90^\circ$, $\theta1 = 90^\circ$ and $E = 0$.

Ra^*	Cavity geometry	
	Square	Circular
10^3	0.5365	0.5488
10^4	0.5500	0.5675
10^5	0.6390	0.6646

VI. CONCLUSIONS

1. A finite element model is formulated, tested and used for steady heat transfer and buoyancy-driven flow within enclosures containing cavities of different geometries.
2. The results show that the effect of wall conductance cannot be neglected.
3. Enclosures with square cavities are shown to be better insulators than those with circular ones for the same wall material and area ration.
4. The assumption, widely used before, of perfectly insulated connecting walls is far from the realistic condition of finite wall conductance.

REFERENCES

- [1] Chan, A.M.C and Banerjee, S., "Three - Dimensional analysis of transient natural convection in rectangular enclosure," *ASME, Jr. of Heat Transfer*, vol. 101, pp. 114-119, 1979.
- [2] El-sherbiny, S.M., Hollands, K.G.T. and Raithby, G.D., "Effect of thermal boundary condition on natural convection in vertical and inclined air layers," *ASME, Jr. of Heat Transfer*, vol. 104, pp. 515-520, 1982.
- [3] Meyer, B.A., Mitchell, J.W., and El-Wakil, M.M., "The effect of thermal wall properties on natural convection in inclined rectangular cells," *ASME, Jr. of Heat Transfer*, vol. 104, pp.111-117, 1982.
- [4] Mallinson, G.D., "The effects of side-wall conduction on natural convection in a slot," *ASME, Jr. of Heat Transfer*, vol. 109, pp.419-426, 1987.
- [5] Kim, D.M. and Viskanta, R., "Effect of wall heat conduction on natural convection heat transfer in square enclosure," *Jr. of Heat Transfer*, vol. 139, pp. 139-146, 1985.
- [6] Baker, A.J., *Finite Element Computational Fluid Mechanics*, McGraw-Hill Book Company, 1983.
- [7] Kim, D.M., "Heat transfer by combined wall conduction, convection and radiation through a solid with cavity;" Ph. D. Thesis, Purdue University, West Lafayette, Indiana, USA, 1983.
- [8] Jones, I.P., "Numerical predictions from the IOTA2 code for natural convection in vertical cavities," *ASME paper*, 82HT-70, 1982.
- [9] Kublbeck, K. and Straub, J., "Numerical computation of two-dimensional time-dependant free convection problem," in *Numerical Solutions for a Comparison Problem on Natural Convection in an Enclosure Cavity*, Edited by Jones, I.P. and Thompson, C.P., AERER9955, HMSO, pp. 89-91, 1981.
- [10] Lauriat, G., "Natural convection in enclosed cavity: A comparison problem," in *Numerical Solutions for a Comparison Problem on Natural Convection in an Enclosure Cavity*, Edited by Jones, I.P. and Thompson, C.P., AERER9955, HMSO, pp. 89-91, 1981.
- [11] Raithby, G.D., and Wong, H.H., "Heat transfer by natural convection across vertical air layers," *Numerical Heat Transfer*, vol. 4, pp. 447-457, 1981.
- [12] Nguyen. D. Dumas, G. and Dhatt, G., "Convection and conduction heat transfer in cavities composed wall," *Numerical Methods in Thermal Problem, Proceedings of the Fourth int. Conf.*, vol. 4, part 1, pp. 412-423, (15-18 1985).
- [13] Fayad, M.A., Fernández-Rodríguez, D., Herreros, J.M., Lapuerta, M., Tsolakis, A., "Interactions between aftertreatment systems architecture and combustion of oxygenated fuels for improved low temperature catalysts activity," *Fuel*, 229, pp. 189-197, 2018.
- [14] Fayad, M.A., Herreros, J. M., Martos, F. J., Tsolakis, A., "Role of Alternative Fuels on Particulate Matter (PM) Characteristics and Influence of the Diesel Oxidation Catalyst," *Environ. Sci. Tech.*, 2015.